DYNAMICAL CHARACTERISTICS OF CIRRUS CLOUDS FROM AIRCRAFT AND RADAR MEASUREMENTS

I. Gultepe and D. O'C. Starr
NASA, GSFC, Code 913 Greenbelt MD 20771
A. J. Heymsfield
NCAR, P.O. Box 3000, Boulder CO 80307
M. Poellot
UND Depart. of Atmos. Sci.
Grand Forks, ND 58202
T. Uttal
NOAA WPL, Marine street, RL6, Boulder CO 80307
T. Ackerman
Pennsylvania State Uni., University Park, PA 16802

1. INTRODUCTION

Cirrus clouds play an important role in climate and in the development of other types of clouds. Although there are many studies of clouds within the boundary layer, cirrus clouds have been neglected up until the last decade. New tools and in-situ measurements of various physical and dynamical parameters permit us to now study cirrus clouds in much greater detail. Physical and dynamical structures of cirrus clouds were studied in detail by Heymsfield (1975) using aircraft measurements. He emphasized the importance of interactions among physical and dynamical processes. Cirrus clouds often exhibit complex physical and dynamical structure. Upper tropospheric flows contain not only coherent structures, but also chaotic movements (Pinus, 1989). The coherent structures (organized movements) transfer significant amounts of heat and momentum while their form, size, and intensity depend strongly on environmental instability (Starr and Wylie, 1990).

In this study, various dynamical structures including cells, waves, and turbulence are studied in order to understand cirrus cloud formation and development.

2. DATA

Data for this study were collected by the NCAR King Air and UND Citation aircraft in conjunction with ground-based PSU 3 mm conventional and NOAA 8.66 mm Doppler radar observations, and radiosondes during FIRE Cirrus-II field project that took place over Kansas. The cases of November 26 and December 6 1991 were studied because of the strong dynamical activity occuring on those days.

Aircraft measurements from the NCAR king Air and UND Citation were sampled at 20 and 24Hz, respectively. The measurements of temperature, wind components, and particle size and concentrations from aircraft were used to analyze the size and intensity of dynamical structures. Aircraft measurements are interpolated to the individual points by a cubic spline technique with 0.05 second time interval.

Measurements of Doppler velocity and backscatter power from a vertical pointing NOAA Doppler radar were also used for the analysis of dynamical activity. The NOAA Doppler radar data were only available for the November 26 case. The PSU radar measurements used only to obtain reflectivity factor were available for both the November 26 and December 6 cases.

Analysis of the NOAA Doppler radar and PSU radar data are described by Uttal et al. (1993).

3. METHOD

a. Coherent structures and fluxes from aircraft measurements

Turbulent heat and momentum fluxes within coherent structures (e.g., cells and waves)

in the upper troposphere can play an important role for cirrus development. Cloud dynamical structure was analyzed for coherence and swirling. Swirling was analyzed at two different scales: 1) less than 1 km and 2) larger than 1 km. Separation of scales is made through the use of a running-average filter technique.

The parameter of vortex spirality (swirling) used to analyze coherent structures is calculated from fluctuations of vertical and horizontal winds collected at constant altitudes. The intensity of spirality (swirling), assuming that the spiral is swirled as a whole, is estimated from the following equation (Pinus, 1989):

$$S_{sw} = \frac{G/2}{1-(G/2)} \tag{1}$$

where $G = \sigma_w/\sigma_u$ and σ_u and σ_w represent the root mean squares (rms) values of horizontal and vertical wind fluctuations. The swirling intensity is divided into the three categories: 1) weak ($S_{sw} < 0.4$), 2) moderate ($0.4 < S_{sw} < 0.6$), and 3) strong ($S_{sw} > 0.6$). Moderate to strong swirling indicates the presence of coherent structures (organized eddies). In additon to the swirling parameter, another indication of the presence of coherent structures is obtained by using the calculation of coherence coefficients. The coherence of two time series is determined by Konyaev (1981) as

$$H(f) = \frac{\overline{c_i(f)c_j^*(f)}}{(\overline{c_i(f)c_i^*(f)}\,\overline{c_j(f)c_j^*(f)})^{0.5}} \tag{2}$$

where the $c_i(f)$ and $c_j(f)$ are the amplitude spectra of time series observed at points i and j, respectively. The $c_{i,j}^*(f)$ is the complex conjugate of $c_{i,j}(f)$. We also use Eq. (2) to identify coherent structures. If the coherence coefficient $H(f)$ between two parameters is greater than 0.15, then vertical and horizontal fluctuations in the turbulent flow are correlated and a coherent structure is present at the corresponding wave number (Pinus, 1989).

Momentum and heat fluxes were calculated using a technique similar to eddy-accumulation technique. In this technique, fluxes of some parameter c are estimated separately for both upward and downward directions and summed as:

$$\overline{c'w'} = \overline{c'w'}^{(+)} + \overline{c'w'}^{(-)} \tag{3}$$

where the left hand side is equal to the net flux over a constant altitude flight leg. The first term on the right hand side of Eq. (3) is the averaged positive flux and the second term of the r.h.s. is the averaged negative flux.

b. Coherent structures from radar measurements

Calculation of the size of the dynamical structures from radar measurements (vertically pointing) is made using reflectivity factor (in dBZ) and Doppler wind measurements. Although vertical air velocity calculation from Doppler radar measurements should be made by subtracting particle terminal velocity from Doppler velocity, here we used Doppler velocity and reflectivity factor to identify the cells (coherent structures). This is sufficient for our purpose of locating cells. Size of the strong reflectivity areas L_r is calculated using the aircraft constant altitude wind measurement (U_h).

c. Vertical velocity estimation

Vertical velocity w obtained from aircraft measurements may include large errors. Therefore, mean values are substracted from measurements at each constant altitude flight leg. Size

of the cells is estimated from coherence analysis and visual analysis of w time series. The w's from the PSU and NOAA radars within the generating cells are estimated using shear region characteristics of falling ice crystals (Marhall and Gordon, 1957). In generating cells, when ice crystals grow large enough, gravity causes the ice crystals to fall and fall streaks occur in the shear region. In this case, terminal velocity V_t is estimated as

$$V_t = (U_h - U_c)\frac{\Delta z}{\Delta s}, \tag{4}$$

where U_c is the cell speed, U_c the wind speed in the shear zone, z the vertical distance, s the distance along streak. Falling conditions of ice crystals occur when V_t is slightly larger than w in the generating cell. As a first approximation, we assume $w \approx V_t$ where w is the vertical motion in the generating cell.

4. RESULTS AND CONCLUSIONS

Results show that the size of coherent structures estimated from aircraft measurements ranged from 0.2 km up to 10 km (Table 1). They were comparable to those found from radar measurements. The w from aircraft measurements at constant altitudes was found between a few cm s^{-1} and 1 m s^{-1} in both small and large mesoscales (see Fig. 1). Vertical velocity within generating cells (see Figure 2) was found to be about 1 m s^{-1}. The swirling coefficient S_{sw}, which also shows degree of coherency, ranged from 0.2 to 1.4 in the large scale and 0.4 to 1.0 in the small scale. The ratio between small scale eddy fluxes and larger mesoscale eddy fluxes was found to be between 0.20 and 0.40 (see Table 2). For upward heat fluxes, the ratio was much higher (0.43) than for the downward heat fluxes (0.27). Eddy size ranged between 2 and 10 km on leg 4 of November 26 (Fig. 3). Gust vectors in Fig. 3 are obtained from fluctuations of w and U_h. A suggested flow pattern is marked by dashed lines. Overall, estimated values of cirrus dynamical characteristics for the November 26 case were found to be more intense than those of the December 6 case.

Acknowledgement: Authors would like to thank Dr. Eugene Clothiaux of PSU in Pennsylvania for generating of radar images. This work was done while first author held a NRC Associateship at NASA/GSFC in Greenbelt Maryland and it is supported by the NASA Office of Space Science and Applications under the director of Dr. John T. Suttles.

REFERENCES

Gultepe, I., and D. O'C Starr, 1993: Dynamical structure and turbulence in cirrus clouds: Aircraft observations during FIRE. *J. Atmos. Sci.*, Accepted.

Heymsfield, A. J., 1975: Cirrus uncinus generating cells and evolution of cirrform clouds: Part II: Structure and circulations of the cirrus uncinus generating head. *J. Atmos. Sci.*, 32, 809-819.

Konyaev, K. V., 1981: *Spectral Analysis of Physical Oceanography Data.* Translated from Russian., Amerind Publishing Co.. New Delhi. 200 pp.

Marshall, J. S., and W. E. Gordon, 1957: Radiometeorology. *Meteorological Res. Rew.*, 3, 73-98.

Pinus, N. Z., and G. N. Shur. 1989: Experimental investigation of the coherent structure of turbulent currents in the lower troposphere. *Soviet Meteor. and Hydrol.*, 5, 19-24.

Starr, D. O'C., and D. P. Wylie, 1990: The 27-28 October 1986 FIRE cirrus case study: Meteorology and clouds. *Mon. Wea. Rev.*, 118, 2259-2287.

Uttal, T., R. A. Cropfli, E. Clothiaux, and T. P. Ackerman, 1993: Comparison of 3 mm and 8 mm radar radar reflectivities. Preprints. *26th Conference on Radar Meteorology.* Norman Oklahama.

$\frac{\lambda}{Leg[Z(km)]}$	10 km	5 km	1 km	0.5 km	0.2 km
1 (6.0)	0.3	*	0.5	0.6	0.4
2 (6.3)	0.1	*	0.4	0.6	*
3 (6.6)	*	0.5	*	0.6	0.7
4 (6.9)	*	0.4	0.4	0.5	*
5 (7.2)	0.3	*	0.5	0.8	*
6 (7.5)	*	0.6	0.9	0.7	0.8
7 (8.8)	0.6	*	0.5	0.6	0.7

Table 1: Coherence values between T and w at constant altitude flight legs for December 6 case. λ is obtained from true air speed and frequency f. Coherence is less than 0.20 is indicated by $\star$.

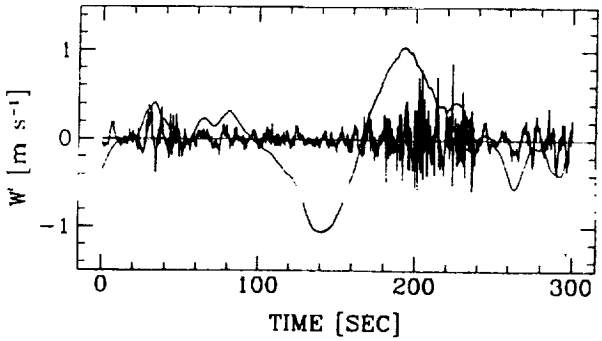

Figure 1: Vertical velocity w fluctuations at 7.3 km. Data are collected from NCAR King Air measurements on 26 November 1991. Aircraft true air speed was $\approx$100 m s^{-1}. Smooth line is for large mesoscale and other one is small mesoscale. Separation of scales is at 1 km.

Leg	R^+_{wT}	R^-_{wT}	R^+_{ww}	R^-_{ww}	R^+_{wu}	R^-_{wu}
1	0.27	0.20	0.24	0.18	0.19	0.10
2	0.33	0.40	0.45	0.41	0.32	0.31
3	0.20	0.05	0.08	0.10	0.07	0.08
4	0.15	0.14	0.18	0.11	0.13	0.14
5	0.06	0.15	0.08	0.24	1.22	1.21
6	1.70	0.83	0.72	0.37	0.59	0.82
7	0.30	0.10	0.25	0.04	0.16	0.14
Mean	0.43	0.27	0.29	0.21	0.38	0.40

Table 2: Ratio R between small and large scale fluxes for upward (+) and downward (-) for December 6 case.

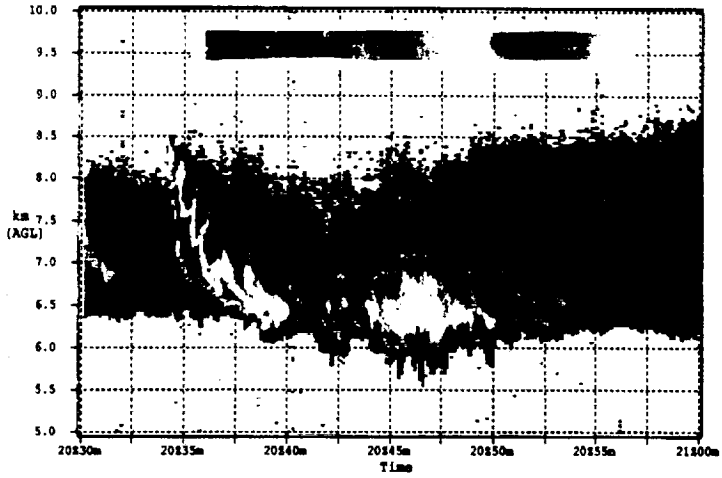

Figure 2: Relative radar reflectivity (dBZ) is obtained from the PSU radar on 26 November 1991.

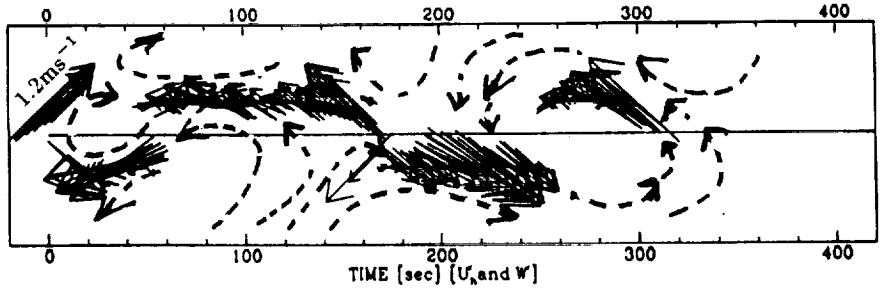

Figure 3: Shows gust vectors obtained from w and U_h wind fluctuations at constant altitude about 7.9 km on November 26, 1991. A suggested flow pattern is marked by dashed lines.